Heliyon 10 (2024) e35889

Contents lists available at ScienceDirect

Heliyon

journal homepage: www.cell.com/heliyon

Research article

Intelligent trapezoid and variable weight combination-based reconstructed GM model

Shanhua Zhang [a], Hong Ki An [b,*], Hongmei Yin [a]

[a] Department of Digital Equipment, Jiangsu Vocational College of Electronics and Information, Huai'an, 223003, China
[b] Faculty of Civil Engineering & Technology, Universiti Malaysia Perlis, Arau Perlis, 02600, Malaysia

ARTICLE INFO

Keywords:
Background value
Genetic algorithm
GM(1.1)
Newton interpolation formula

ABSTRACT

The GM(1,1) model's prediction accuracy is significantly influenced by the accuracy of background value estimation. The traditional trapezoidal background value can only be applied to a specific data sequence. Therefore, this study proposes a GM(1,1) model background value reconstruction approach based on the combination of intelligent trapezoidal and variable weights in order to increase the model's application as well as its prediction accuracy. The trapezoidal background value function with slope and point position parameters is called model I. Then, a set of point position parameter sequences, with a new background value function is constructed, called model II. A genetic algorithm is utilized to seek for the values of the parameters to be determined in both models I and II. The results showed that for the exponential growth data series, model I and II have higher prediction accuracy compared to traditional models. For data sequences, taking the traffic volume series of a road from 2014 to 2023, the prediction accuracy of this paper's model I method can be improved by 0.3643 % and 0.2725 % compared with Deng's and Wang's models. The prediction accuracy of this paper's model II method has been further improved by 0.1075 % compared with that of model I.

1. Introduction

In 1982, "Systems and Control Letters" from North-Holland Publishing Company published the first grey systems. "The Control Problems of Grey systems" by Chinese scholar Professor Deng, marking the beginning of grey systems [1]. System theory is the official birth of an emerging discipline [2]. After more than 30 years of development, its practicality has been widely demonstrated. The main application of grey system theory in prediction is the GM(1,1) model. Since the GM(1,1) model requires fewer sample data and easy to calculate, it has been widely used in transportation, energy, hydrology, ecology, environment, military, society, economy, and many other scientific fields [3–5]. However, the conventional GM(1,1) model frequently falls short of the requirements regarding the accuracy of prediction and data adaptability because of the algorithm's flaws. Therefore, to increase the model's forecast, many scholars are studying grey prediction from different angles. A number of optimization research has been conducted on the model to increase its predictive accuracy and applicability, mainly from numerical transformation generation [6–9], improvement of boundary value conditions [2,10,11], improvement of background values [12,13], improvement of model parameter estimation methods [14], optimization of residual sequences [15,16] comprehensive optimization [17–20] and other aspects.

Among them, the background value is a key factor influencing the prediction accuracy of the GM(1,1) model [21]. Assuming that

* Corresponding author.
E-mail addresses: 201203@jsei.edu.cn (S. Zhang), hongkian@unimap.edu.my (H.K. An), 022105@jsei.edu.cn (H. Yin).

https://doi.org/10.1016/j.heliyon.2024.e35889
Received 29 March 2024; Received in revised form 30 July 2024; Accepted 6 August 2024
Available online 8 August 2024

the monotonicity of the non-negative original sequence $X^{(0)} = \{x^{(0)}(k)\}_{k=1,\dots,n}$, $X^{(0)}$ tends to be inconspicuous and random, which is not conducive to the analysis and computation of the data, while one-additive preprocessing can lessen the data's unpredictability and enhance the regularity of the data. Therefore, in this paper, $X^{(0)}$ is accumulated once to get $X^{(1)}$, and the processing method is shown in equations. (1) and (2).

$$x^{(1)}(k) = \sum_{i=1}^{k} x^{(0)}(i), k = 1, \cdots, n \tag{1}$$

$$X^{(1)} = \{x^{(1)}(k)\}_{k=1,\dots,n} \tag{2}$$

Since the sequence $X^{(1)}$ increases monotonically, it is useful for modeling and data analysis. Any two adjacent index values k-1 and k, with the index value as the abscissa, the index corresponding value $x^{(1)}(k)$ as the ordinate, Draw the two points $(k\text{-}1, x^{(1)}(k-1))$ and $(k, x^{(1)}(k))$ as illustrated in Fig. 1. The background value in the geometric meaning is the area enclosed by line segment A k-1, line segment k-1 k, line segment k B and curve BA. Since the equation of curve BA is unknown, and the actual background value cannot be obtained through integration. Thus, in Ref. [1] proposed a combination of the line segment A k-1, the line segment k-1 k, the line segment k B and the line segment BA. The classic background value calculation formula's source of error is the size of the contained trapezium, which is utilized as an estimate of the background value, as well as the area enclosed by the curve AB and the line segment AB. Therefore, in order to eliminate background value errors, scholars have done a number of research on background value reconstruction. However, current studies on background values have "static" problems and cannot dynamically change the background value estimation with different sequences.

Therefore, it is necessary to use intelligent algorithms to dynamically optimize the background value parameters. Typical intelligent algorithms with similar principles include the GA (Genetic Algorithm) and the PSO (Particle Swarm Optimization) algorithms. These two algorithms have been widely used in the field of optimizing parameters of objective functions [22,23]. In the GA algorithm, chromosomes share information with each other, so the entire population moves relatively uniformly towards the optimal region. In PSO, particles share information only through the current best point found, so to a large extent, it is a one-way information-sharing mechanism. The entire search and update process follows the current optimal solution. From this perspective, the PSO algorithm can converge to the optimal solution faster than the GA algorithm. However, this also makes the PSO algorithm more prone to getting stuck in local optima. GA has been developed for a longer time and already has mature convergence analysis methods. Compared to the PSO algorithm, the GA algorithm has a broader applicability [24]. To better accommodate various data types, this paper adopts the GA algorithm to determine the parameters to be optimized.

Currently, biomimetic intelligent algorithms and artificial intelligence algorithms have been widely applied to the field of parameter determination and prediction. These include the Multistart Nelder-Mead neural network algorithm [25], Genetic Nelder-Mead neural network algorithm [26], Adaptive Quasi-Monte Carlo Method for Nonlinear Function Error Propagation algorithm [27], Improved Artificial Gorilla Troops Optimizer with Chaotic Adaptive Parameters [28], Memristor-based artificial neural networks algorithm [29], particle swarm optimization-backpropagation-artificial neural network algorithm [30], Wavelet Transform (WT) and Particle Swarm Optimization Support Vector Machine (PSO-SVM) algorithms [31], the combination of backpropagation neural network optimized by genetic algorithm (GA-BP) and support vector machine (SVM) algorithms [32], hybrid genetic algorithm and modified support vector machine classifier [33], and so on. Some of the aforementioned research uses a single intelligent algorithm, but most of them combine multiple intelligent algorithms for optimization, improving the adaptability or robustness of the algorithms. These methods have significant guiding importance for this study, which aims to combine and optimize multiple algorithms. However, artificial intelligence algorithms mainly rely on large data samples, which are not suitable for this study's small sample data. Therefore, previous artificial intelligence algorithms are not appropriate for this study. Instead, this study attempts to combine biomimetic intelligent algorithms with the GM(1,1) model, using biomimetic intelligent algorithms to determine the undetermined parameters in

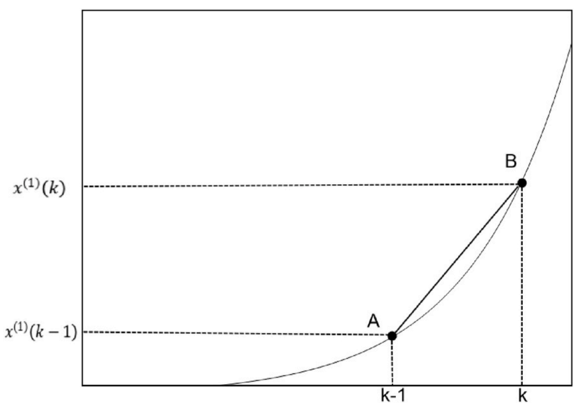

Fig. 1. The concept of background values.

the GM(1,1) model and applying the optimized GM(1,1) model for prediction.

In recent years, the process of urban integration in China has accelerated, leading to an increasing demand for travel and worsening traffic congestion. The urban issues caused by traffic congestion have become major factors affecting the economic development of cities. Therefore, how to solve traffic congestion has attracted widespread attention from researchers in various fields [34–36]. Furthermore, traffic volume forecasting is key to taking effective measures to alleviate traffic congestion. Traffic volume forecasting can be divided into medium- and long-term, and short-term forecasts based on the prediction interval duration [37,38]. Medium- and long-term traffic volume forecasting uses intervals of days, months, or even years, and is typically used for situations requiring macro-level traffic volume predictions, such as traffic planning. This paper mainly focuses on urban medium- and long-term traffic volume forecasting. Thus, a method that can improve the effectiveness of existing forecasting methods has always been a focus of traffic management research.

For the reasons mentioned above, this paper presents a suitable method of intelligent trapezoidal construction, which is applicable to all types of data. First, the 1-AGO data sequence polynomial function is approximated by quadratic Newton interpolation formula and the trapezoid is constructed by using polynomial function. Second, a Genetic Algorithm (GA) is introduced into the estimation of trapezoidal background value to adapt to various types of data changes, and the key parameters in trapezoidal construction are searched for by the GA. Finally, it has been verified that this method has good prediction accuracy for exponential growth data, and it can also be used to predict the actual road traffic volume.

2. Literature review

Currently, there is extensive research on traffic volume forecasting, primarily based on machine learning algorithms, including Bayesian network models [39], neural network models [40], and support vector machine models [41]. Zhu [39] proposed using a Bayesian clustered Gaussian process ensemble model for prediction. This model performs hard clustering on input data based on a Dirichlet process mixture model; within each cluster, it uses Gaussian processes to learn the probabilistic relationship between inputs and outputs. During the prediction phase, the model performs soft clustering on the inputs as weights and predicts using the weighted average of the Gaussian process outputs. Manikandan [40] employed deep convolutional neural networks and used TensorFlow to predict traffic flow from real-time traffic data at different locations. The application of computer-based TensorFlow in deep neural networks verifies the accuracy of the algorithm. Toan [41] proposed an effective method for short-term traffic flow prediction using support vector machines and compared it with two traditional methods. The model was trained and tested using one month of time series traffic flow data from a section of Singapore's Pan-Island Expressway, validating the algorithm's effectiveness.

The aforementioned studies are all based on machine learning algorithms for traffic volume prediction, extending the research depth in the field of traffic volume forecasting and improving the prediction accuracy of the models. However, these models share a common issue: they rely on large sample data due to the use of machine learning algorithms. In practical traffic volume forecasting applications, small sample data may exist, rendering machine learning algorithms ineffective for accurate prediction. The GM(1,1) model, due to its advantages of requiring fewer sample data and simpler calculations, can be applied in this field.

There has been quite a lot of research on GM(1,1) model background value optimization and the main purpose is to construct a new background value expression. In Ref. [42] defined the accumulation sequence as a homogeneous exponential function, starting with the background value's geometric meaning. It derived a new background value calculation formula and increased the model's prediction accuracy. However, the one-time accumulation sequence is a non-homogeneous exponential function. In Ref. [43], further optimized the background value calculation algorithm and developed the one-time accumulation sequence as a non-homogeneous exponential function. In Refs. [44,45], further optimized based on the above background value calculation formula. The GM(1,1) model's prediction accuracy and applicability are both enhanced by the aforementioned technique. However, the above background value calculation formula does not consider the geometric significance of constructing the background value, resulting in prediction accuracy that still needs further improvement. At the same time, the proposed background value calculation formula also constrains the model's applicable range and cannot be dynamically adjusted according to changes in the original sequence.

In [46,47], the analysis highlighted the significance of constructing background values in the GM(1,1) model. Reasonably constructing background values can improve the accuracy and adaptability of the grey model. The paper discussed methods for reconstructing background values in the GM(1,1) model based on data interpolation and numerical integration using Newton-Cotes formulas. Simulation examples verified the effectiveness of the proposed methods. Zhu et al. [48] approached the construction of background values from a geometric perspective, using a monotonic piecewise cubic spline interpolation reconstruction curve to improve the background values and enhance the prediction accuracy of the grey model. Cheng et al. [49] used optimized values of exponential functions, power functions, polynomial functions, and difference functions as background values within the original model structure to calculate the parameters of the GM(1,1) model, aiming to improve prediction accuracy. Ma et al. [50] proposed a new discrete GM(1,1) model, where the background values were reconstructed using Simpson's formula. They derived the expression of the specific time response function, and the proposed model was proven to be unbiased, capable of simulating homogeneous exponential sequences, and validated with actual sequences.

The aforementioned methods all optimized the traditional trapezoidal background value from a geometric perspective. However, in Refs. [46–50], most methods used numerical integration combined with the accumulated sequence scatter values to construct a function that approximates the accumulated sequence, obtaining the time response sequence equation. This type of model, on the one hand, requires complex mathematical knowledge, making the model construction process quite complicated. On the other hand, the GM(1,1) model, optimized using numerical integration approximation, can only adapt to specific sequences. For some sequences, the improvement in prediction accuracy may be insignificant, or the prediction performance may even deteriorate.

Wang [51] further optimized the model by considering the geometric significance of the background values. Using the Lagrange mean value theorem, he constructed the background values as variables related to k, and set the initial values as variables. The corresponding optimal parameters and time response formula were determined based on the minimum average relative error. By applying this method to domestic annual natural gas consumption data, the accuracy of the grey model's predictions was improved. These methods enhance the adaptability of the model to data by incorporating undetermined parameters into the construction of background values and solving for these parameters. However, the aforementioned models use traditional mathematical methods for solving, which have drawbacks such as slow solving speed, complexity in computation, and low precision of results. In today's era of rapid computer development, intelligent algorithms are a very good choice.

Liu [52] used the composite mean value theorem of integration to reconstruct the dynamic background values of the fractional grey model and proposed a variable background value based on the fractional grey model. Specifically, the particle swarm optimization algorithm (PSO) was then used to determine the optimal values of the fractional order and background value coefficients. The model's effectiveness was validated using electricity consumption data from Beijing and Inner Mongolia as examples. This model introduced undetermined parameters into the construction of background values and used the PSO algorithm to determine the optimal values of these undetermined parameters, improving the accuracy of background value construction. However, there is a background value function between any two adjacent index values $k-1$ and k, and each function has different trends. This means that using a single undetermined parameter cannot make all the background value functions completely approximate the actual values, indicating that there is still room for improvement in the prediction accuracy of the GM (1,1) model.

In [53], optimized the traditional trapezoidal background value and transformed the background value into an arithmetic weighting to increase the model's flexibility for various data sequences, and $z^{(1)}(k)$ has a background value of $ax^{(1)}(k-1)+(1-a)x^{(1)}(k)$. It determined the optimal parameter a through theoretical analysis and iteration method. In Ref. [54], used GA to search and determine the value of the optimal parameter a, which further improved the model's prediction accuracy. The model's applicability can be greatly increased by optimizing the background value using the unknown parameter a and by employing intelligent algorithms for searching to find the optimum parameter value. However, there are still two problems in the above research. First, the weighted sum of the adjacent data, $x^{(1)}(k-1)$ and $x^{(1)}(k)$, is used to calculate the traditional trapezoidal background value calculation algorithm. This trapezoidal background value construction method has great limitations and is difficult to adapt to different change sequences. Secondly, the background value is a sequence set $\{z^{(1)}(k)\}_{k=2,\dots,n}$, and all background value sequence element values are estimated using a specific background value parameter. It can only achieve comprehensive optimization but cannot lessen the error between the actual each background value and the estimated background value. Therefore, serializing the values of the undetermined parameters in the background value function will make the background value estimate closer to the actual background value and improved the model's prediction accuracy. The determination of the undetermined set elements is a key factor influencing the model's prediction accuracy. According to the above study, intelligent algorithms have better results in determining background value parameters. Therefore, this study attempts to use GA to calibrate and improve an undetermined set of parameter sequences.

In summary, the main contributions of this paper are as follows:

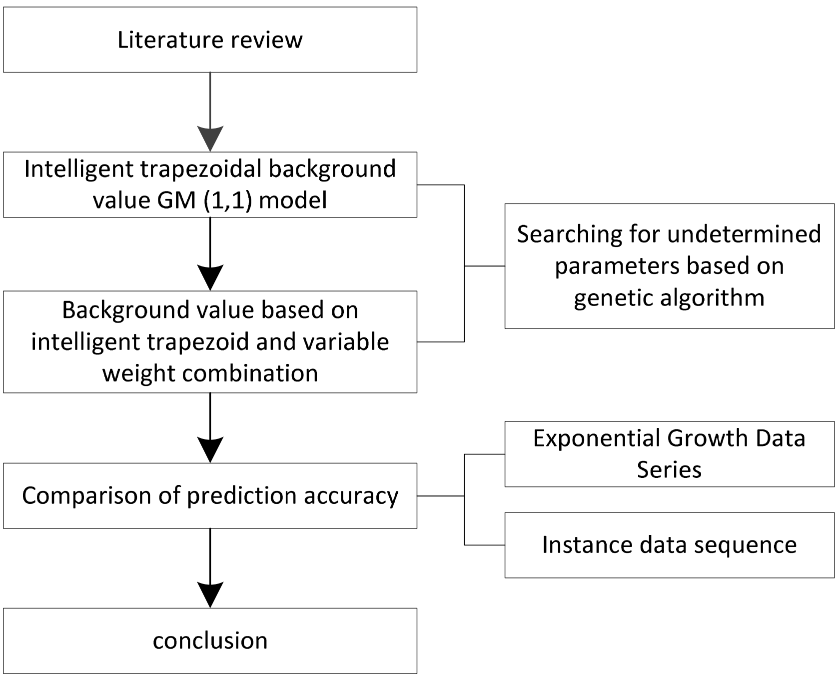

Fig. 2. Research flowchart.

- Based on the traditional trapezoidal background value construction, this paper establishes a new trapezoidal background value function containing two undetermined parameters using simple mathematical geometric thinking. Compared to traditional optimization approaches, the new trapezoidal background value construction is simpler, does not rely on complex mathematical theories, and offers higher prediction accuracy.
- This paper proposes two new GM(1,1) models with optimized background values. The background value function includes two undetermined parameters: the point position parameter and the slope parameter. The optimal values of these parameters are obtained using the GA (genetic algorithm). The GM(1,1) model with this background value is designated as Model I. Based on Model I, the undetermined parameters undergo variable weight optimization, making the values of the position and slope parameters dependent on the index value k, varying with k. This further improves the accuracy of the background value function. The optimal parameter set is obtained using the GA genetic algorithm, and the GM(1,1) model with this background value is designated as Model II.
- Validation with exponential data sequence examples shows that the two new GM(1,1) models proposed in this paper have higher prediction accuracy compared to traditional models and can adapt to rapid data growth.

3. Research methods

This study proposes and examines a GM(1,1) model background value reconstruction method based on the combination of variable weights and intelligent trapezoidal in the following steps, as described in Fig. 2. First step, the traditional GM(1,1) model optimization method was analyzed through literature review. To facilitate the determination of the study direction, research topics pertaining to background value optimization will be identified from this review. Second step, in terms of GM(1,1) model, an intelligent trapezoidal background value with undetermined parameters is constructed using the background value's geometric meaning. In the third stage, the variable weights of the undetermined parameters are combined in order to improve the prediction accuracy of the GM(1,1) model. A background value is then created by combining the intelligent trapezoid with the variable weights. After that, use GA to find the optimum value for each of the undetermined parameters in the background value function. Finally, a comparison between the two proposed GM(1,1) models (Model I and II) and the two conventional GM(1,1) models is conducted: one is Deng [1] model hereinafter referred to as Deng's model and the other one is Wang [54] model hereinafter referred to as Wang's model, the exponential growth data sequence and the instance data sequence are used for verification respectively.

4. Background values for smart trapezoidal and variable weight combinations

4.1. Construction of polynomial functions approximating 1-AGO data sequence polynomials based on quadratic Newton interpolation Formulation

A series of discrete points is formed from the sequence of $X^{(1)}$ and its corresponding transverse coordinate values (k-values). The functional equation and the function value between any two points (k-1, $x^{(1)}(k-1)$) and (k, $x^{(1)}(k)$) ($2 \leq k \leq n-1$) are unknown. Therefore, smart trapezoids cannot be constructed to estimate the background values. Due to the computational simplicity and good approximation of Newton's interpolation formula [55], and the number of interpolations is too high will cause the Runge phenomenon, i.e., The quadratic Newton's interpolation formula is used to construct the polynomial function, and the difference formula is shown in Definition 1.

Definition 1. Assume that any four different k1, k2, k3 and k4 function values of f(k_1), f(k_2), f(k_3) and f(k_4) in the function f(x); that is:

- The first order difference between k_i and k_j is divided into:

$$f[k_i, k_j] = \frac{f(k_i) - f(k_j)}{k_i - k_j} \tag{3}$$

- The second-order difference between k_i, k_j and k_l is divided into:

$$f[k_i, k_j, k_l] = \frac{f[k_j, k_l] - f[k_i, k_j]}{k_l - k_i} \tag{4}$$

- The third order difference between k_1, k_2, k_3 and k_4 is divided into:

$$f[k_1, k_2, k_3, k_4] = \frac{f[k_2, k_3, k_4] - f[k_1, k_2, k_3]}{k_4 - k_1} \tag{5}$$

Property 1. *The difference value is independent of the order of the nodes, i.e.*:

$$f[k_{i1},k_{i2},\cdots,k_{in}]=f[k_1,k_2,\cdots,k_n] \tag{6}$$

where [ki1, ki2, …, kin] is any permutation of [k1, k2, …, kn].

Theorem 1. Assume three points (k-1, x(1)(k-1)), (k, x(1)(k)) and (k+1, x(1)(k+1)) 2≤k ≤ n-1 in X(1) and set N2(t) ≈x(1)(t)(t∈ [k-1, k]). The Newton interpolation polynomial function in the interval [k-1, k] is then:

$$x^{(1)}(t)=x^{(1)}(k-1)+\left(x^{(1)}(k)-x^{(1)}(k-1)\right)\cdot(t+1-k)$$
$$+\left(\frac{1}{2}x^{(1)}(k-1)-x^{(1)}(k)+\frac{1}{2}x^{(1)}(k+1)\right)\cdot(t+1-k)\cdot(t-k)$$

Proof. Suppose $t\in[k\text{-}1,k]$; according to definition 1, $f[t,k-1]=\frac{x^{(1)}(t)-x^{(1)}(k-1)}{t-k+1}$. Determine $x^{(1)}(t)$ as shown in equation (7).

$$x^{(1)}(t)=f[k-1,t]\cdot(t-k+1)+x^{(1)}(k-1) \tag{7}$$

According to definition 1, $f[t,k-1,k]=\frac{f[k-1,k]-f[t,k-1]}{k-t}$. Determine f [$k$-1, t] as shown in equation (8).

$$f[k-1\ ,\ ,t]=f[k-1,k]+(t-k)\cdot f[k-1,k,t] \tag{8}$$

Where f [t, k-1] = f [k-1, t] by Property 1.

According to definition 1, $f[t,k-1,k,k+1]=\frac{f[k-1,k,k+1]-f[t,k-1,k]}{k+1-t}$. Determine $f[k-1,k,t]$ as shown in equation (9).

$$f[k-1,k,t]=f[k-1,k,k+1]+(t-k-1)\cdot f[t,k-1,k,k+1] \tag{9}$$

Where, it can be concluded that f [k-1, k, t] = f[t,k-1,k] according to property 1. Equations (8) and (9) are brought into the upper equation in turn, which can be expressed in equation (10).

$$\begin{aligned}x^{(1)}(t)=x^{(1)}(k-1)+f[k-1,k]\cdot(t+1-k)\\+f[k-1,k,k+1]\cdot(t+1-k)\cdot(t-k)\\+f[k-1,k,k+1,t]\cdot(t+1-k)\cdot(t-k)\cdot(t-k-1)\end{aligned} \tag{10}$$

Where $N_2(t)=x^{(1)}(k-1)+(t-k+1)\cdot f[k-1,k]+(t-k+1)\cdot(t-k)\cdot f[k-1,k,k+1]$. N_2(t) is a quadratic Newton interpolation polynomial function, $R(t)=(t-k+1)\cdot(t-k)\cdot(t-k-1)\cdot f[k-1,k,k+1,t]$, and $R(t)$, is the remainder of quadratic Newton interpolation polynomial function. This is because according to definition 1, $N_2(t)\approx x^{(1)}(t)$, ($t\in[k-1,k]$), the difference quotient values f[k-1, k] and f[k-1, k,k+1] are introduced into N_2(t) for simplification to obtain equation (11).

$$x^{(1)}(t)=x^{(1)}(k-1)+\left(x^{(1)}(k)-x^{(1)}(k-1)\right)\cdot(t+1-k)+\left(\frac{1}{2}x^{(1)}(k-1)-x^{(1)}(k)+\frac{1}{2}x^{(1)}(k+1)\right)\cdot(t+1-k)\cdot(t-k)\quad(t\in[k-1,k]) \tag{11}$$

End of proof.

For example, in a first-order accumulated sequence with three adjacent points (1, 1357), (2, 2385), and (3, 4006), assuming $N_2(t)\approx x^{(1)}(t)(t\in[1,2])$, calculate the Newton interpolation polynomial function over the interval [1,2]. Substitute the given variables into

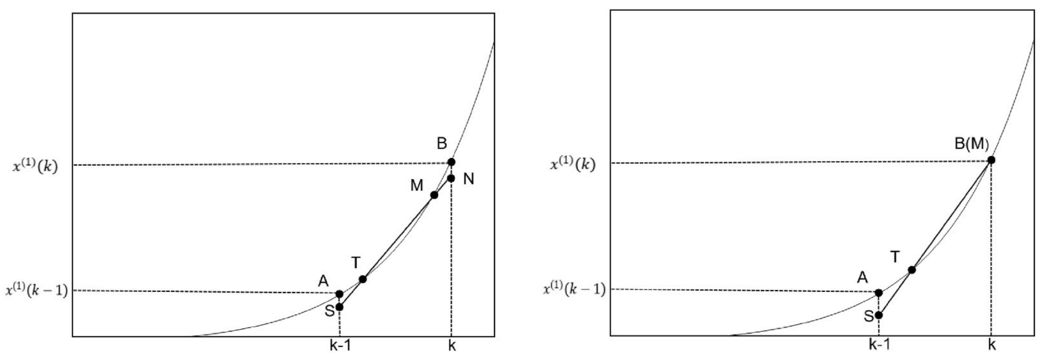

(a) Background value function construction graph (b) Plot of the effect of the background value function of the point B coinciding with the point M

Fig. 3. Ladder background value function construction diagram.

equation (11), where k is 2, $x^{(1)}(k-1)$ is 1357, $x^{(1)}(k)$ is 2385, and $x^{(1)}(k+1)$ is 4006. Ultimately, solving yields $x^{(1)}(t) = 2681.5\cdot t^2 - 7016.5\cdot t + 5692 (t \in [1,2])$.

4.2. Optimization of background values

4.2.1. Construction of the background value of the smart trapezoid

With coordinates of $(t, x^{(1)}(t))$ (k-1$\leq t < k$), take any point T on curve AB, the value of $x^{(1)}(t)$ is given by equation (11). Draw a straight line through point T and intersect curve AB at another point M, as shown in Fig. 3(a). When point M coincides with point B, the slope of the line TB is as shown in equation (12) as shown in Fig. 3(b).

$$k_{TB} = \frac{x^{(1)}(k) - x^{(1)}(t)}{k-t} \tag{12}$$

Where k_{TB} is the slope of line TB, the slope of line TM is less than the slope of line TB, which means that the slope of line TM can be expressed as $\partial\cdot k_{TB}(0 \leq \partial \leq 1$, $\partial$is the slope parameter) and that line TM passes the point T. Then, the function of line TM is as shown in equation (13). When point T is determined, the slope change effect diagram of straight-line TM is shown in Fig. 4.

$$y - x^{(1)}(t) = \partial\cdot\left(\frac{x^{(1)}(k) - x^{(1)}(t)}{k-t}\right)\cdot(x-t) \tag{13}$$

The line in transverse coordinates equal to *k-1* intersects with *k* at two points *S* and *N*. To solve for the value of the function of the line *TM* at *k-1* and *k*, substitute the transverse coordinates of *k-1* and *k* into equation (13).

When $x = k-1$.

$$y_{k-1} = \partial\cdot\left(\frac{x^{(1)}(k) - x^{(1)}(t)}{k-t}\right)\cdot(k-1-t) + x^{(1)}(t) \tag{14}$$

when$x = k$.

$$y_k = \partial\cdot\left(\frac{x^{(1)}(k) - x^{(1)}(t)}{k-t}\right)\cdot(k-t) + x^{(1)}(t) \tag{15}$$

Where y_{k-1} and y_k are the function values of line *TM* at the abscissae of *k*-1 and *k*, y_{k-1} and y_k are as the upper line and down line of a trapezoid. The new background value function value is the trapezoid area surrounded by line segment *S k-1*, line segment *k-1 k*, line segment *k N* and line segment *N S*. Equation (16) shows the estimation function of the background value based on the trapezoidal area.

$$z^{(1)}(k) = 0.5\cdot(y_{k-1} + y_k) = x^{(1)}(t) + \partial\cdot\left(\frac{x^{(1)}(k) - x^{(1)}(t)}{k-t}\right)\cdot\left(k - t - \frac{1}{2}\right) \tag{16}$$

Where the point *T* is any point in the interval [k-1, k] on the curve, which indicates that the abscissa of point *T* can be represented as $t = k\text{-}1 + d$ ($0 \leq d < 1$, d is the point position parameter). Then, take the abscissa of point *T* into equation (16), and obtain equation (17).

$$z^{(1)}(k) = 0.5\cdot(y_{k-1} + y_k) = x^{(1)}(k-1+d) + \partial\cdot\left(\frac{x^{(1)}(k) - x^{(1)}(k-1+d)}{1-d}\right)\cdot\left(\frac{1}{2} - d\right)$$
$$(0 \leq \partial \leq 1, 0 \leq d < 1, 2 \leq k \leq n-1) \tag{17}$$

Substituting the expression of $x^{(1)}(t)$ in equation (11) into equation (17), then equation (18) can be obtained.

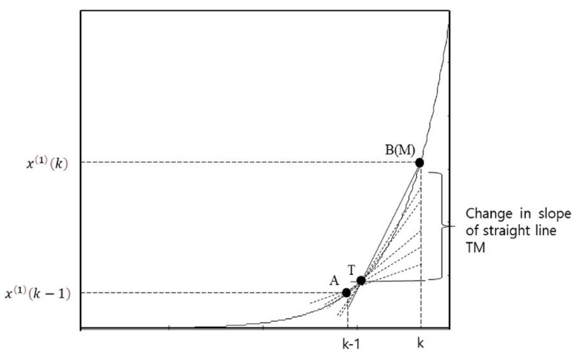

Fig. 4. Linear TM slope change effect graph.

$$\begin{gathered}z^{(1)}(k)=x^{(1)}(k-1)+\left(x^{(1)}(k)-x^{(1)}(k-1)\right)\cdot(d+\partial\cdot(1/2-d))\\ +d\cdot\left(1/2\cdot x^{(1)}(k-1)-x^{(1)}(k)+1/2\cdot x^{(1)}(k+1)\right)\cdot(d-1-\partial\cdot(1/2-d))\\ (0\leq\partial\leq 1,0\leq d<1,2\leq k\leq n-1)\end{gathered} \tag{18}$$

The background value for intelligent trapezoid construction can be calculated using equation (18). When $d = 0$ and $\partial = 1$, equation (18) is the background value of the classic GM(1,1) model [1], so the background value of the excellent GM(1,1) includes the classic GM(1,1) model background value, the GM(1,1) model constructed by equation (18) is defined as model I. The above equation contains two undetermined parameters, ∂ and d, with a maximum degree of 3 (cubic equation). This background value function is a bivariate cubic nonlinear function. Because it is not a conventional function, exploring its monotonic characteristics using mathematical methods is quite complex. Therefore, using intelligent algorithms for optimization is a very good choice.

4.2.2. Variable weight optimization of intelligent trapezoidal background values

The following equation shows the calculation of the traditional approach of trapezoidal background value in Deng's model.

$$z^{(1)}(k)=\frac{1}{2}\cdot\left(x^{(1)}(k)+x^{(1)}(k-1)\right),k=2,..,n \tag{19}$$

The following equation shows Wang's model's background value calculating procedure.

$$z^{(1)}(k)=ax^{(1)}(k-1)+(1-a)x^{(1)}(k),k=2,..,n \tag{20}$$

In this study, the optimized background value calculation approach is based on equation (18) and performs variable weight optimization on the slope parameter ∂ and the point position parameter d. The calculation method is shown in the following equation.

$$\begin{gathered}z^{(1)}(k)=x^{(1)}(k-1)+\left(x^{(1)}(k)-x^{(1)}(k-1)\right)\cdot(d(k)+\partial(k)\cdot(1/2-d(k)))\\ +d(k)\cdot\left(1/2\cdot x^{(1)}(k-1)-x^{(1)}(k)+1/2\cdot x^{(1)}(k+1)\right)\cdot(d(k)-1-\partial(k)\cdot(1/2-d(k)))\\ (0\leq\partial(k)\leq 1,0\leq d(k)<1,2\leq k\leq n-1)\end{gathered} \tag{21}$$

Among them, $\left\{z^{(1)}(k)\right\}_{k=2,\dots,n-1}$ is the background value sequence, $\{\partial(k)\}_{k=2,\dots,n-1}$ is the slope parameter sequence, $\{d(k)\}_{k=2,\dots,n-1}$ is the point position parameter sequence. In order to increase the precision of the model prediction and the accuracy of the background value estimate, the optimization idea of this study is to gather the unknown parameters in the background value function and convert them into weight sequences. The GM(1,1) model constructed by equation (21) is called model II.

4.3. Modeling steps for optimizing the GM(1,1) model

Let the original data non-negative sequence be : $X^{(0)} = \left\{x^{(0)}(1),x^{(0)}(2),\dots,x^{(0)}(n)\right\}$.

Perform an accumulation calculation on $x^{(0)}$ to obtain the sequence $X^{(1)} = \left\{x^{(1)}(1),x^{(1)}(2),\dots,x^{(1)}(n)\right\}$, the main calculation method is as shown in equation (1).

The grey differential equation of GM(1,1) model is shown in the following equation (22).

$$x^{(0)}(k)+a\cdot z^{(1)}(k)=u,k=2,\dots,n-1 \tag{22}$$

The parameters a and u are parameters in GM(1,1) model modeling, and the calculation method can be expressed in equation (23).

$$(a,u)^T=\left(B^TB\right)^{-1}B^TY \tag{23}$$

In, $B=\begin{bmatrix}-Z^{(1)}(2) & 1\\ -Z^{(1)}(3) & 1\\ & \cdots\\ \cdots-Z^{(1)}(n-1) & 1\end{bmatrix}$, $Y=\begin{bmatrix}X^{(0)}(2)\\ X^{(0)}(3)\\ \cdots\\ X^{(0)}(n-1)\end{bmatrix}$, the calculation methods of the background value sequence $\left\{z^{(1)}(k)\right\}_{k=2,\dots,n-1}$ are as shown in equations (18) and (21) respectively. Equation (24), which illustrates the whitening equation of the grey differential equation of the GM(1,1) model, is derived based on the GM(1,1) modeling principle.

$$\frac{dx^{(1)}}{dt}+a\cdot x^{(1)}=u \tag{24}$$

The time response sequence of an accumulation sequence can be found by solving the whitening differential equation, as indicated by equation (25).

$$\widehat{x}^{(1)}(k)=\left(x^{(1)}(1)-\frac{u}{a}\right)\cdot e^{-a\cdot(k-1)}+\frac{u}{a},k=1,\dots,n \tag{25}$$

Among them, $\widehat{x}^{(1)}(k)$ is a cumulative prediction sequence, $\widehat{x}^{(1)}(1) = x^{(1)}(1)$.

The cumulative reduction value is shown in the following equation (26).

$$\hat{x}^{(0)}(k) = \hat{x}^{(1)}(k) - \hat{x}^{(1)}(k-1) = (1 - e^{a}) \cdot \left(x^{(1)}(1) - \frac{u}{a}\right) \cdot e^{-a\cdot(k-1)}, k = 1, \dots, n \tag{26}$$

Where $\hat{x}^{(0)}(k)$ is the original prediction sequence.

According to the modeling steps, one significant influencing parameter that the GM(1,1) model can predict is the determination of the slope and point location parameters. Thus, the following describes how to determine the background value undetermined parameter.

4.4. Determination of background value parameters based on GA

As a highly efficient optimization method seeking a global, optimal solution without any initialization information, GA can be effectively combined with various algorithms and applied to many fields [56]. It has been common practice to search the GM(1,1) background value parameter using GA [57,58]. GA is used to intelligently search the optimum important parameters of trapezoid background value estimation in this paper.

4.4.1. Chromosome coding and initial population generation

Chromosome coding: The key undetermined parameters of a trapezoid building background function are slope parameter and point position parameter. To make selection, cross mutation and other operations more convenient, binary coding is adopted [59]. For model I, there are two undetermined parameters in the background value function. The encoding length ω is set to 20 to achieve more than three decimal places accuracy for the parameters ∂ and d in the search process. The first 10 binary code length represents parameter ∂, while the latter 10 binary code length represents parameter d. For Model II, the number of undetermined parameters in the background value function is determined based on the original sequence number n, and the number of undetermined parameters is $2(n-2)$. Each parameter occupies a 6-bit binary encoding length, and the encoding length ω is $12(n-2)$. The precision τ of each number encoding can be determined by equation (27).

$$\tau = \frac{\sigma_{\max} - \sigma_{\min}}{2^{\varpi} - 1} \tag{27}$$

where ϖ represents the encoding length of a binary number; $\sigma_{\max}$ and $\sigma_{\min}$ indicate the range of decimal numbers of undetermined parameters, the value of $\sigma_{\max}$ and $\sigma_{\min}$ are 1 and 0. τ represents the precision of encoding for each undetermined parameter. This value reflects the search accuracy of the genetic algorithm. For example, if the search precision for the undetermined parameter values needs to be accurate to two decimal places or more, then $\tau \le 0.01$. The coding of the decimal value represented in the GA can be obtained by converting coding binary to the decimal number and then multiplying by the number of encoding accuracy.

Initial population generation: Generate N initial populations at random. The population size is generally between ω and 2ω. In model I, the population size is 40, while in model II, it is $24(n-2)$ and this allows for a faster convergence to the optimal solution.

4.4.2. Calculation of the fitness function

An individual's fitness within the population is often determined as the GA's objective function. The fitness function is the main basis of "survival of the fittest" in the future. The individual with a large fitness has a higher chance of transferring their genes to the next generation. In contrast, a person with low fitness has a reduced likelihood of transferring their genes to the next generation. Equation (28), which calculates the average relative error, is used in this study to identify the background value's critical parameters that result in the lowest average relative error.

$$e_r = \frac{1}{n} \sum_{k=1}^{n} \frac{\left|\hat{x}^{(0)}(k) - x^{(0)}(k)\right|}{\left|x^{(0)}(k)\right|} \tag{28}$$

Where e_r is the average relative error predicted by the GM(1,1) model, and $\hat{x}^{(0)}(k)$ is the predicted value. The corresponding slope parameter and point position parameter values of each individual population are introduced into the background value estimation equation. The GM(1,1) model is solved to obtain the corresponding predicted sequence. $x^{(0)}(k)$ is the actual value, and n represents the amount of data in a sequence. Equation (29), which represents the fitness function of the GA, uses the reciprocal of the average relative error to reach agreement with the highest value of the GA's fitness function.

$$f_{fitnessfunction} = n \cdot \sum_{k=1}^{n} \frac{\left|x^{(0)}(k)\right|}{\left|\hat{x}^{(0)}(k) - x^{(0)}(k)\right|} \tag{29}$$

4.4.3. Operations of selection, crossover and mutation

Selection Generally, a high level of fitness increases the likelihood that an individual will pass on their genes to the next generation. To establish the relationship between individual fitness and individual survival probability, the probability that each person will survive is calculated using the Monte Carlo method. It is the link to establishing the relationship between individual fitness and individual survival probability as shown in equation (30).

$$P_j = \frac{f_j}{\sum_{i=1}^{N} f_i} j = 1, 2, \cdots, N \tag{30}$$

Where P_j is for the survival probability of individual j, f_j stands for the fitness function value of individual j, and N is the number of individuals in the population.

The roulette method uses a fan area to divide the roulette wheel and is based on the survival probability found using the Monte Carlo method. A larger P_j corresponds to a greater area on the roulette wheel. The specific operation of the roulette method is as follows: A bamboo stick is fixed at the center of the roulette wheel, and every time the bamboo stick is rotated, the individual whose area the bamboo stick has stopped in is selected. At the same time, the same operation would be carried out N times to obtain N new individual populations.

Crossover: It is the process of creating a new individual by partially recombining and replacing the structural components of two parent individuals. An essential component of the GA is the crossover operator. Single-point crossover is utilized, and the crossover probability is typically 0.4–0.99, to minimize the time complexity of the crossover portion. Thus, this study selects 0.6 for better prediction results. The specific process of crossover is: perform crossover operation on any two adjacent individuals. First, judge whether to crossover based on probability. If not, the two individuals will not change. If crossover is performed, then select the intersection point and exchange the codes after the intersection point, as shown in Fig. 5 before and after cross transformation.

Mutation: A mutation is a shift in the gene values of individual strings within the population at specific loci, to maintain the diversity of individuals in the population and prevent them from falling into local optimality. The mutation probability pm is usually taken as 0.0001–0.1. This study refers to the previous study [34] where the mutation probability pm is taken as 0.001. The specific process of mutation is: select mutant individuals based on probability, and select mutation points on the selected individuals. If the original gene is 1, it becomes 0, and if the original gene is 0, it becomes 1.

The fitness calculation, selection, crossover and mutation procedures are repeatedly carried until the predetermined number of iterations (100 iterations in this study) is fulfilled or a satisfactory result is obtained. The choice of iteration count primarily depends on the convergence of the algorithm. By observing the effect graph of the fitness function as it changes with the number of iterations, when the fitness function stabilizes with increasing iterations and approaches a steady value, it is recognized that the algorithm has converged. The iteration count corresponding to algorithm convergence is recorded. Through multiple experiments, the maximum iteration count corresponding to stable convergence is selected as the iteration count for the experiments in this paper.

5. Result and discussion

5.1. Modeling and testing of exponential growth data series

The optimization method in this study is utilized to predict exponential growth sequences using the GM(1,1) model, an approximate exponential fitting method. The parameter a is the development coefficient in the GM(1,1) model, as shown in equation (22). Thus, the exponential growth data sequence is calculated and generated by the following equation (31).

$$x^{(0)}(i) = e^{-a(i-1)}, i = 1, 2 \cdot \cdot, 6 \tag{31}$$

Where, i is the index sequence number; -α is taken as 0.2,0.4,0.6,0.8,1.0,1.2,1.4,1.6,1.8,2.0 for simulation analysis. Table 1 shows the resulting of original sequence.

This study compared models I and II with Deng's model and Wang's model, and GM(1,1) model is built with the background value of model I by applying the method in Wang's model for data sequences under various development coefficients. For data sequences under different development coefficients, the optimal background value searched by GA is used. The parameters that need to be

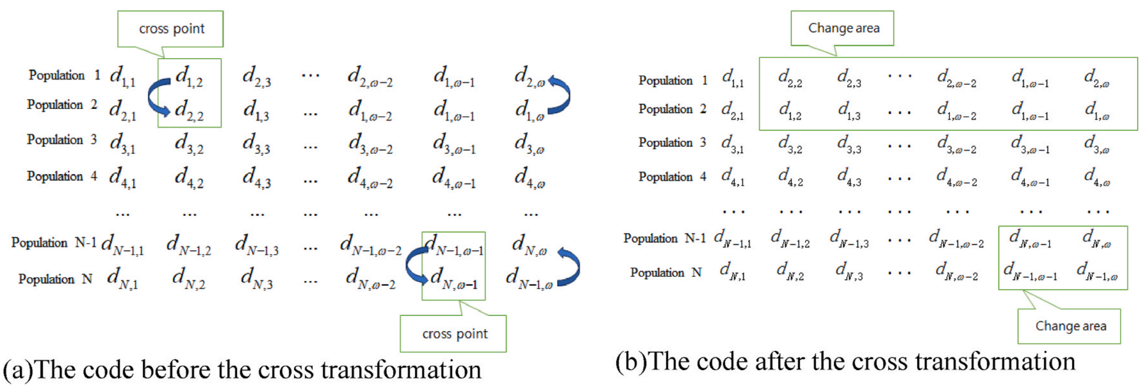

Fig. 5. Cross processes.

Table 1
Exponential growth series with different development coefficients.

i / $\lvert a \rvert$	1	2	3	4	5	6
0.2	1	1.2214	1.4918	1.8221	2.2255	2.7183
0.4	1	1.4918	2.2255	3.3201	4.9530	7.3890
0.6	1	1.8221	3.3201	6.0496	11.0232	20.0855
0.8	1	2.2255	4.9530	11.0232	24.5325	54.5982
1.0	1	2.7183	7.3891	20.0855	54.5982	148.4132
1.2	1	3.3201	11.0232	36.5982	121.5104	403.4288
1.4	1	4.0552	16.4446	66.6863	270.4264	1096.6331
1.6	1	4.9530	24.5325	121.5104	601.845	2980.958
1.8	1	6.0496	36.5982	221.4064	1339.4308	8103.0839
2.0	1	7.3891	54.5982	403.4288	2980.958	22026.4658

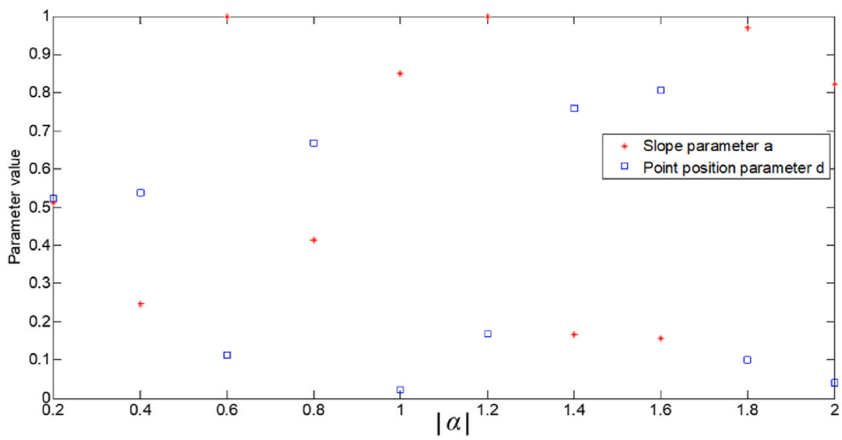

Fig. 6. Optimal background value weights obtained based on model I searching.

determined are depicted in Fig. 6. Also, this paper creates a GM(1,1) model on the basis of the Model II background value. For data sequences under different development coefficients, the optimal background value undetermined parameter sequence searched by the GA is illustrated in Fig. 7.

Fig. 6 illustrates that when the GA converges, the values of the slope parameter ∂ and point position parameter d are obtained by searching under different development coefficients. The parameters have no obvious change rules, and the scattered points are randomly distributed. In order to predict the outcomes, the parameter will be substituted into equation (18) together with the GM(1,1) model.

According to Fig. 7, it can be seen that when the GA converges, the values of the slope parameter sequence $\partial(i)$ and the point position parameter sequence $d(i)$ are obtained by searching under different development coefficients. The parameter value scatter points are randomly distributed, and there is no obvious changing pattern of it. The prediction results can be derived by entering the parameter sequence into equation (21) and combining it with the GM(1,1) model.

The four GM(1,1) models use the undetermined parameters obtained from the above research to substitute into the background value function and combine with the modeling steps to calculate the prediction results, as shown in Fig. 8.

When the development coefficient $|a| = 0.2$, the four GM(1,1) model's forecast outputs essentially match the actual values. As the development coefficient increases, the prediction results of Deng's model deviate more and more from the actual values. When the development coefficient is greater than 1 and the index value i is greater than 4, from the graph, it can be visually observed that there is a significant deviation between the prediction and the actual values. As the development coefficient changes, the prediction results of the other three methods basically coincide with the actual values, indicating that the two models proposed in Wang's model and this study have high prediction accuracy. The prediction results are entered into the following equation (32) to determine the relative error at each point, allowing for a more accurate comparison of the three approaches' forecast accuracy.

$$e(k) = \frac{\left|\hat{x}^{(0)}(k) - x^{(0)}(k)\right|}{\left|x^{(0)}(k)\right|} \tag{32}$$

where $\hat{x}^{(0)}(k)$ is the predicted value, $x^{(0)}(k)$ is the actual value, and $e(k)$ is the relative error value.

The relative error value can be calculated by using the predicted and actual values from Fig. 8 into equation (32). The development coefficient $|a|$, the index sequence number i and the corresponding relative error are sorted to form a spatial error point. For better

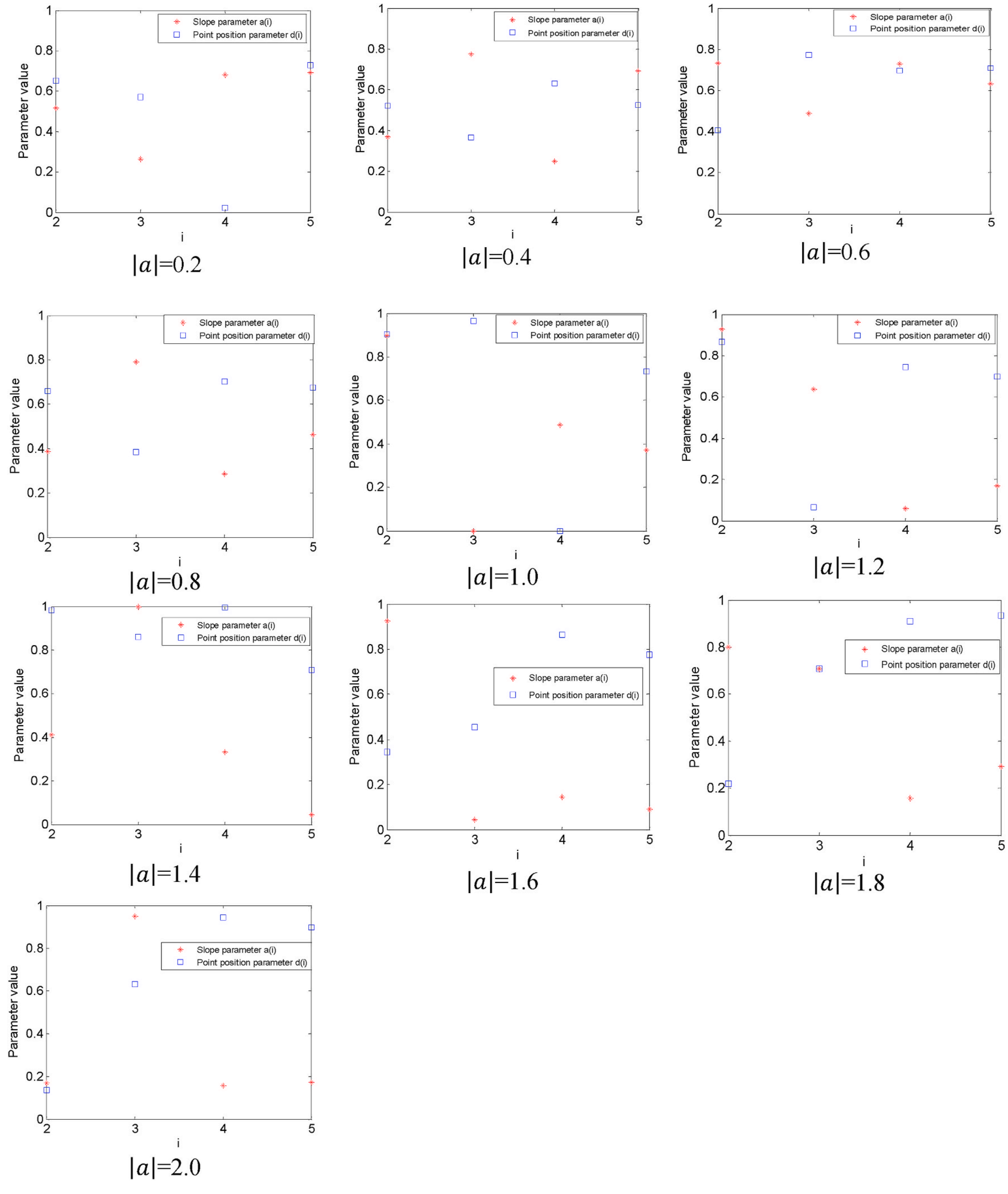

Fig. 7. Optimal background value weights obtained based on the Model II search.

observation the relative error values under different development coefficients, different index sequence numbers and convert the points into surfaces through interpolation. The relative error surface plots predicted by the four GM(1,1) models are shown in Fig. 9.

The "." shown in Fig. 9 calculates the relative error value scatter points for equation (32). The relative error of the GM(1,1) model on the basis of Deng's model increases with the increase of the development coefficient. The interval [0,1] contains the relative errors for each scatter point. The prediction result is distorted, When the development coefficient |a| is greater than 1. This is the same as the analysis result in Fig. 8. Based on Wang's model, the relative error from the GM(1,1) model has no obvious relationship with the development coefficient and the change of index sequence number *i*. All relative errors are within the interval [0,0.00004]. When the development coefficient takes 1.8 and the index sequence number *i* takes 2, the relative error reaches the maximum value, and the space surface exists. There are multiple extreme points, and the relative error in most areas is within 0.000015. Wang's model provides

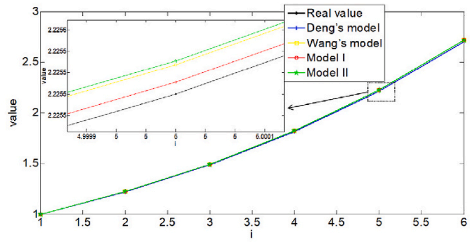

$|a|=0.2$

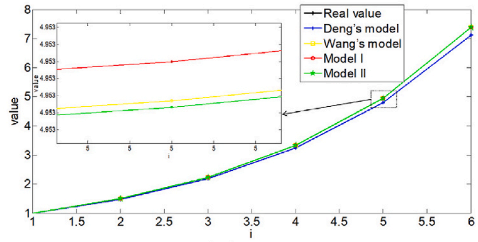

$|a|=0.4$

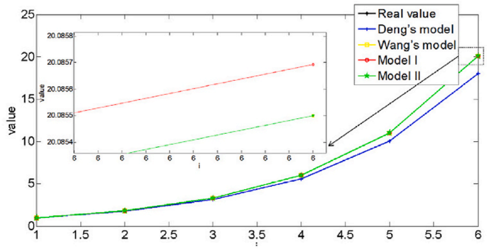

$|a|=0.6$

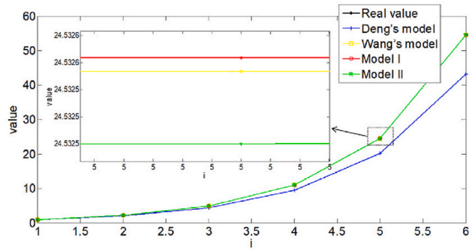

$|a|=0.8$

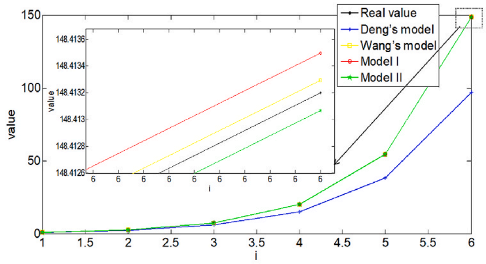

$|a|=1.0$

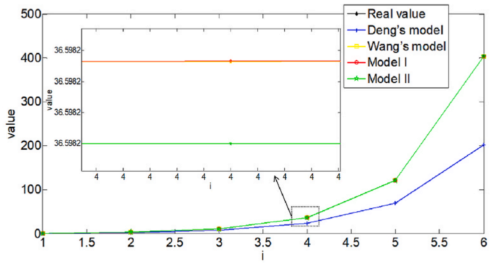

$|a|=1.2$

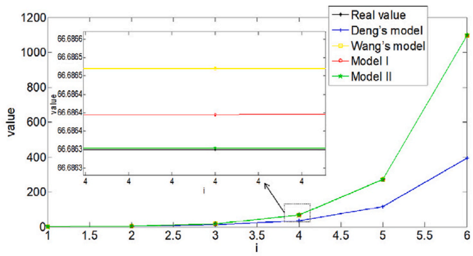

$|a|=1.4$

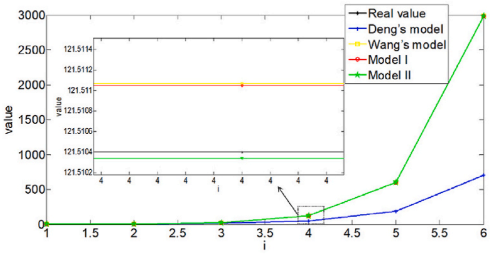

$|a|=1.6$

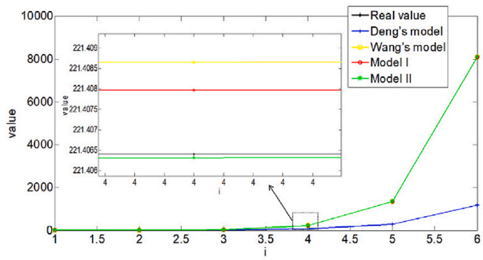

$|a|=1.8$

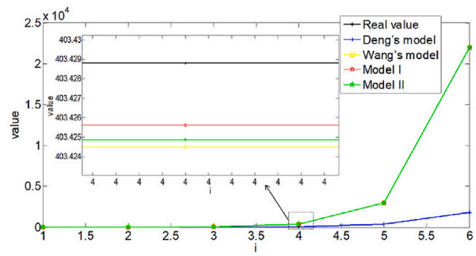

$|a|=2.0$

Fig. 8. Predicted and actual values of four GM(1,1) models under different development coefficients.

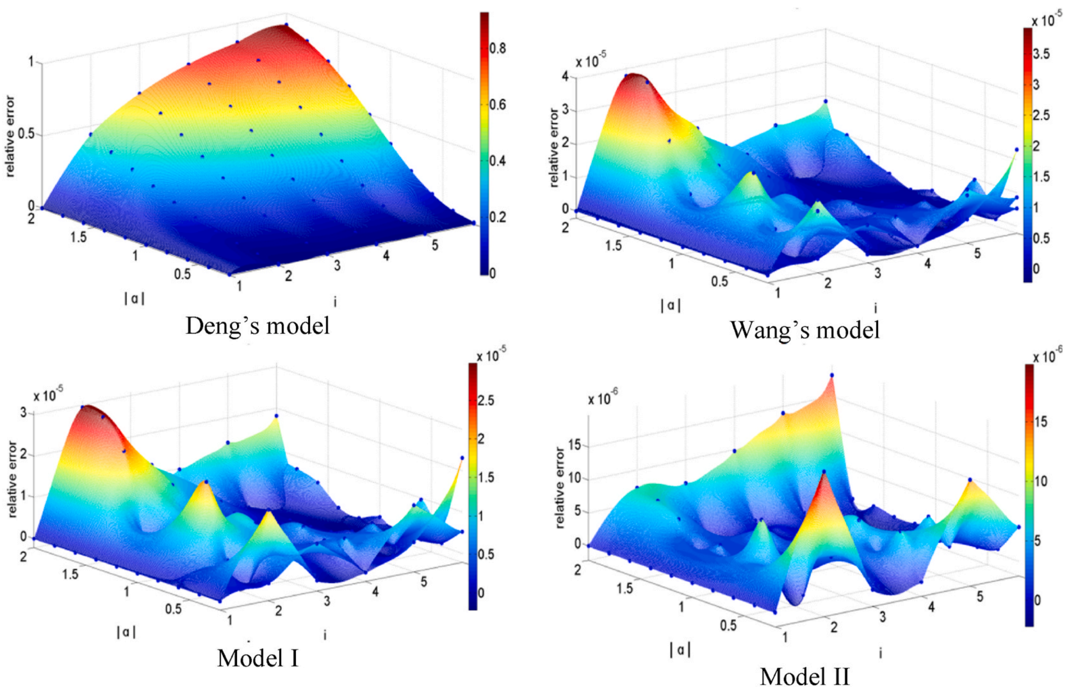

Fig. 9. Relative error surfaces of the predictions of the four GM(1,1) models.

a high prediction accuracy with the GM(1,1) model and can be used to forecast exponential sequences; the relative error and development coefficient based on the model I have no relationship with the change of the index sequence number *i*, and the spatial surface. There is a similar trend to Wang's model. All relative errors are within the interval [0, 0.00003]. When the development coefficient is 2.0 and the index sequence number *i* is 2, the relative error reaches the maximum value. There are multiple extreme points on the space surface, and the relative error in most areas is within 0.00001. Thus, model I is more suitable for exponential sequence prediction than the GM(1,1) model in Wang's model. The relative error based on model II also has no obvious relationship with the development coefficient and the change of index sequence number *i*. All relative errors are within the interval [0,0.00002]. When the development coefficient is 0.2 and the index sequence number *i* is 2, and the relative error reaches the maximum value. There are multiple extreme points on the space surface, and the relative error in most areas is within 0.000005. Therefore, Model II is more suitable for exponential sequence prediction than Model I.

In order to make a better comparison between the four model's approaches' accuracy of prediction, the parameter average relative error of the prediction model is usually used to measure it. Under the same development coefficient, the relative errors corresponding to different index sequence numbers are substituted into equation (28) to obtain the average relative error as summarized in Table 2.

In accordance with the prediction results in the above table, Deng's model has the lowest prediction accuracy. If the development coefficient increases, the average relative prediction error becomes larger and larger. If the development coefficient $|a|$ is greater than 1, the prediction error is more than 20 % and cannot be used for exponential sequence prediction; In Wang's model, the model's prediction accuracy has significantly increased. The lowest prediction accuracy is found at 2.0 for the development coefficient. At this time, the average relative error is 1.35×10^{-3}. It still has high prediction accuracy and can be used for indices. Sequence prediction;

Table 2
Average relative error of four GM(1,1) model predictions (unit: %).

Model / $\|a\|$	Deng's model	Wang's model	Model I	Model II
0.2	0.42	6.56×10^{-4}	6.56×10^{-4}	6.56×10^{-4}
0.4	2.18	3.03×10^{-4}	2.47×10^{-4}	2.39×10^{-4}
0.6	5.9	3.04×10^{-4}	3.73×10^{-4}	1.83×10^{-4}
0.8	11.8	5.06×10^{-4}	5.58×10^{-4}	2.62×10^{-4}
1.0	19.62	3.74×10^{-4}	4.19×10^{-4}	1.19×10^{-4}
1.2	28.66	1.33×10^{-4}	1.33×10^{-4}	1.17×10^{-4}
1.4	38.01	3.86×10^{-4}	1.69×10^{-4}	5.48×10^{-5}
1.6	46.83	7.63×10^{-4}	7.45×10^{-4}	9.58×10^{-5}
1.8	54.55	1.32×10^{-3}	9.61×10^{-4}	1.21×10^{-4}
2.0	60.94	1.35×10^{-3}	1.03×10^{-3}	9.28×10^{-4}

model I's prediction accuracy has been considerably enhanced. When the development coefficient $|a|$ is 2.0, the prediction accuracy is the lowest. At this time, the average relative error is 1.03×10^{-3}, and it still has high prediction accuracy. It can be used for exponential sequence prediction. Compared with the model in Wang's model, except when the development coefficient $|a|$ is 0.6, 0.8 and 1.0, the other prediction accuracy is lower than that of Model I. The main reason analysis in Fig. 8 involves observing the line charts of predicted results under three scenarios of the development coefficient $|a| = 0.6$, 0.8, and 1.0. When the development coefficient $|a|$ is 0.6, upon zooming into the local area at index $i = 6$, Wang's model predictions and Model II predictions closely match the actual values, while Model I predictions show significant deviation from the actual values. This is the primary reason for the lower prediction accuracy of Model I compared to Wang's model when $|a| = 0.6$. Similarly, when the development coefficient $|a|$ is 0.8, upon zooming into the local area at index $i = 5$, Model II predictions closely match the actual values, while Wang's model predictions are closer to the actual values compared to Model I predictions. This is why Model I has lower prediction accuracy than Wang's model when $|a| = 0.8$. Likewise, when the development coefficient $|a|$ is 1.0, upon zooming into the local area at index $i = 6$, Wang's model predictions are closer to the actual values compared to Model I predictions. This explains why Model I has lower prediction accuracy than Wang's model when $|a| = 1.0$. In general, compared to Wang's model, Model I has a greater overall accuracy; Model II has the highest prediction accuracy. When the development coefficient $|a|$ is 2.0, the prediction accuracy is the lowest. At this time, the average relative error is 9.28×10^{-4} and it still has high prediction accuracy and can be used for exponential sequence prediction. Compared with other methods, after the development coefficient $|a|$ is determined, the prediction accuracy of model II in this paper is the highest. Among the four GM(1,1) models for exponential sequence prediction, model II in this study has the highest accuracy, followed by model I, followed by model in Wang's model, and finally model in Deng's model.

5.2. Modeling and test of instance data sequences

A certain road annual average daily traffic volume sequence from 2014 to 2023 in Huai'an city was used as the object of study and the original sequence is shown in Table 3. In terms of prediction and verification, four GM(1,1) models were employed, and the GA was used to search for undetermined parameters.

The average relative errors corresponding to the final convergence of the three GM(1,1) models are different, and the prediction accuracies of several GM(1,1) models are further analyzed below. Wang's model searched for the weights a of 0.5324; Model I of this paper searched for the slope parameter ∂ of 0.9254 with the point location parameter d of 0.9999; and the sequence of pending parameters of Model II of this paper is shown in Fig. 10.

Fig. 10 presents that there is no obvious change pattern between the slope parameter sequence $\partial(i)$ and the position parameter sequence $d(i)$ obtained through the search. The undetermined parameters are substituted into the GM(1,1) model, and the predicted results are shown in Fig. 11.

The initial sequence is an approximately monotonically rising sequence, with a mutation point at 2015 on the abscissa. Model I and Model II are closer to this mutation point than Deng's model and Wang's model, ensuring prediction accuracy. For other points, Model I and Model II should be as close as possible while ensuring their own growth trends, and ensure comprehensive prediction optimization on the basis of discarding the prediction accuracy of some points (such as point 2023).

In summary, compared to the other models, the predicted values of the model I and II in this paper are similar to the field data. Equation (28) shows that the actual value and the predicted value in the figure are combined to get the average relative prediction error of each method, which is shown in Table 4.

The methods by Deng and Wang are compared with model I for prediction accuracy, which can be improved by 0.3643 % and 0.2725 %, respectively, verifying the GM constructed with intelligent trapezoidal background values. For the sudden drop in traffic volume in 2015, Deng's model and Wang's model could not adapt to such data changes. This is the main reason why the overall prediction accuracy is lower than that of Model I. The model is able to enhance the prediction accuracy of actual sequences compared with traditional models. Compared with the Model I method, the prediction accuracy of the Model II method is further improved by 0.1075 %, which verifies that the prediction accuracy can be further improved by using the GM(1,1) model with variable weight optimization of intelligent trapezoidal background values. Combining the analysis of Fig. 11 and Table 4, the main reason Model II achieved better prediction results than Model I is that for the sudden drop in traffic volume in 2015, Model I excessively pursued the prediction accuracy of individual mutation points, leading to a significantly lower overall prediction accuracy for other years compared to Model II. On the other hand, Model II, by adopting a variable weight background value construction approach, ensures the prediction accuracy for both the mutation point year and other years, resulting in Model II's overall prediction accuracy being superior to Model I.

6. Conclusion

This study fits the original sequence based on the quadratic Newton interpolation formula and combines geometric ideas to

Table 3
The traffic volume in a certain road from 2014 to 2023 (unit: vehicles/day).

Year	2014	2015	2016	2017	2018	2019	2020	2021	2022	2023
Volume	1982	1792	2311	2785	2987	3497	4109	4602	5242	5643

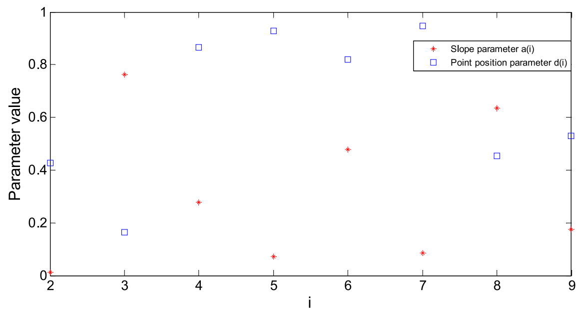

Fig. 10. Values of the sequence of parameters to be determined for the model II of this paper.

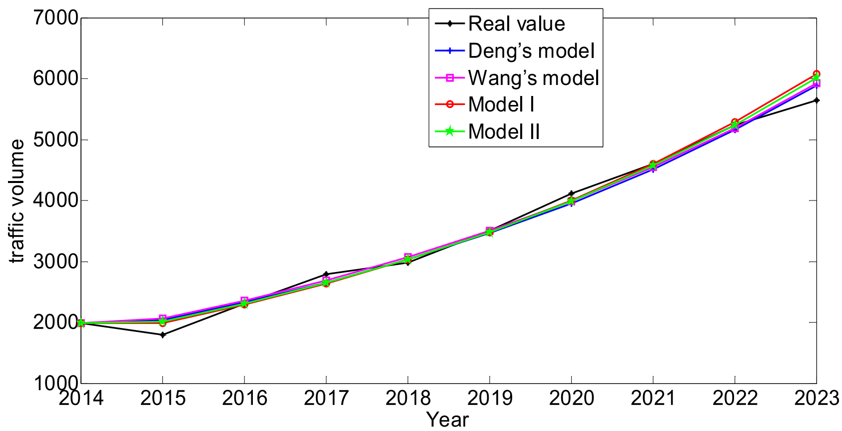

Fig. 11. Prediction results of four GM(1,1) models.

Table 4
Mean relative errors of predictions of four GM(1,1) models.

Method	Deng's model	Wang's model	Model I	Model II
Forecast error	3.4246 %	3.3328 %	3.0603 %	2.9528 %

construct the trapezoid, which contains point position parameters and slope parameters. For the background value calculation formula, two models are proposed. Firstly, the GM(1,1) model constructed using the new background value function is called model I. Secondly, based on the new background value function, the point position parameters and slope parameters are serialized. Also, a new background value function based on intelligent trapezoid and variable weight combinations is proposed, called Model II. In order to improve the applicability and prediction accuracy of the two GM (1,1) models, a GA is used to intelligently search for the optimal values of the undetermined parameters in the background value function.

In the data simulation prediction, using the exponential growth data sequence as the original sequence, compared with the traditional Deng's model, the models I and II in this paper are better than the Deng's model. For Model II, regardless of the value of the development coefficient, the prediction accuracy of Model II is better than Wang's model. For the actual data sequence, taking the road traffic volume from 2014 to 2023 as the original sequence, the prediction accuracy of the model I method in this paper is 0.3643 % and 0.2725 % higher than the prediction accuracy of Deng's and Wang's models, respectively. Compared with Model I, the prediction accuracy of Model II is further improved by 0.1075 %. The comparison of simulation and prediction accuracy shows that the trapezoidal background value containing point position parameters and slope parameters is able to increase the prediction accuracy of the GM(1,1) model. Moreover, background value function based on intelligent trapezoid and variable weight combination can further improve the GM(1,1) model prediction accuracy. Thus, it can be expected that the proposed methods will serve as a foundation for more in-depth research in the future that focuses on using the GM(1,1) model to forecast time series with accuracy. However, there are some limitations in that the incomplete use of information could influence the accuracy of the model's predictions. Thus, deeper research will be needed on the approximation of 1-AGO data sequences to avoid the situation in which the background value dimension becomes smaller.

Data availability statement

All data generated or analyzed during this study are included in this published article.

Funding

This work was funded by Construction project of "Excellent Science and Technology Innovation Team in Jiangsu Province Universities, China" advanced manufacturing technology team for electronic precision molds; 2022 The General Program of Philosophy and Social Science Research in Colleges and Universities in Jiangsu Province (Grant no. 2022SJYB1969); Jiangsu Vocational College Student Innovation and Entrepreneurship Training Program Project (Grant no. G-2023-0312).

CRediT authorship contribution statement

Shanhua Zhang: Writing – original draft, Software, Resources, Methodology, Funding acquisition, Formal analysis, Data curation, Conceptualization. **Hong Ki An:** Writing – review & editing, Supervision, Conceptualization. **Hongmei Yin:** Visualization, Validation, Resources, Formal analysis.

Declaration of competing interest

The authors declare the following financial interests/personal relationships which may be considered as potential competing interests: Shanhua Zhang reports article publishing charges was provided by Jiangsu Vocational College of Electronics and Information. If there are other authors, they declare that they have no known competing financial interests or personal relationships that could have appeared to influence the work reported in this paper.

References

[1] J.L. Deng, Control problems of grey systems, Systems and Control Letters 1 1 (1982) N0, https://doi.org/10.1016/S0167-6911(82)80025-X.
[2] Y. Dang, S. Liu, K. Chen, The GM models that x (n) be taken as initial value, Kybernetes 33 (2) (2004) 247–254, https://doi.org/10.1108/03684920410514175.
[3] L. Wang, J. Sun, Q. Wu, Nonlinear total least-squares variance component estimation for GM (1, 1) model, Geodesy and Geodynamics 12 (3) (2021) 211–217, https://doi.org/10.1016/j.geog.2021.02.006.
[4] W. Qian, J. Wang, An improved seasonal GM (1, 1) model based on the HP filter for forecasting wind power generation in China, Energy 209 (2020) 118499, https://doi.org/10.1016/j.energy.2020.118499.
[5] B. Zeng, Y. Yang, X. Gou, Research on physical health early warning based on GM(1,1), Comput. Biol. Med. 143 (2022) 105256, https://doi.org/10.1016/j.compbiomed.2022.105256.
[6] J. Li, W. Dai, H. Pan, GM (1, 1) model-ameliorated based on genetic algorithm and its application, in: Third International Conference on Natural Computation (ICNC 2007), vol. 4, IEEE, 2007, August, pp. 23–27, https://doi.org/10.1109/ICNC.2007.407.
[7] C. Li, Y. Yang, S. Liu, A new method to mitigate data fluctuations for time series prediction, Appl. Math. Model. 65 (2019) 390–407, https://doi.org/10.1016/j.apm.2018.08.017.
[8] J. Chen, Z. Wu, A positive real order weakening buffer operator and its applications in grey prediction model, Appl. Soft Comput. 99 (2021) 106922, https://doi.org/10.1016/j.asoc.2020.106922.
[9] X. Gou, B. Zeng, Y. Gong, Application of the novel four-parameter discrete optimized grey model to forecast the wastewater discharged in Chongqing China, Eng. Appl. Artif. Intell. 107 (2022) 104522, https://doi.org/10.1016/j.engappai.2021.104522.
[10] T.L. Tien, A new grey prediction model FGM (1, 1), Math. Comput. Model. 49 (7–8) (2009) 1416–1426, https://doi.org/10.1016/j.mcm.2008.11.015.
[11] S. Ding, R. Li, Forecasting the sales and stock of electric vehicles using a novel self-adaptive optimized grey model, Eng. Appl. Artif. Intell. 100 (2021) 104148, https://doi.org/10.1016/j.engappai.2020.104148.
[12] S. Li, Y. Chen, R. Dong, A novel optimized grey model with quadratic polynomials term and its application, Chaos, Solit. Fractals X (8) (2022) 100074, https://doi.org/10.1016/j.csfx.2022.100074.
[13] Z.X. Wang, Y.G. Dang, S.F. Liu, Optimization of background value in GM (1, 1) model, Systems engineering-theory & practice 28 (2) (2008) 61–67, https://doi.org/10.1016/S1874-8651(09)60011-9.
[14] J. Cui, S.F. Liu, B. Zeng, N.M. Xie, A novel grey forecasting model and its optimization, Appl. Math. Model. 37 (6) (2013) 4399–4406, https://doi.org/10.1016/j.apm.2012.09.052.
[15] X. Yang, S. Wang, Y. Peng, J. Chen, L. Meng, Short-term photovoltaic power prediction with similar-day integrated by BP-AdaBoost based on the Grey-Markov model, Elec. Power Syst. Res. 215 (2023) 108966, https://doi.org/10.1016/j.epsr.2022.108966.
[16] Y.C. Hu, Energy demand forecasting using a novel remnant GM (1, 1) model, Soft Comput. 24 (18) (2020) 13903–13912, https://doi.org/10.1007/s00500-020-04765-3.
[17] M.U. Yousuf, I. Al-Bahadly, E. Avci, A modified GM (1, 1) model to accurately predict wind speed, Sustain. Energy Technol. Assessments 43 (2021) 100905, https://doi.org/10.1016/j.seta.2020.100905.
[18] A.M. Khan, M. Osińska, Comparing forecasting accuracy of selected grey and time series models based on energy consumption in Brazil and India, Expert Syst. Appl. 212 (2023) 118840, https://doi.org/10.1016/j.eswa.2022.118840.
[19] X. Zhu, Y. Dang, S. Ding, Using a self-adaptive grey fractional weighted model to forecast Jiangsu's electricity consumption in China, Energy 190 (2020) 116417, https://doi.org/10.1016/j.energy.2019.116417.
[20] H. Huang, Z. Tao, J. Liu, J. Cheng, H. Chen, Exploiting fractional accumulation and background value optimization in multivariate interval grey prediction model and its application, Eng. Appl. Artif. Intell. 104 (2021) 104360, https://doi.org/10.1016/j.engappai.2021.104360.
[21] Y. Wang, Y. Dang, Y. Li, S. Liu, An approach to increase prediction precision of GM (1, 1) model based on optimization of the initial condition, Expert Syst. Appl. 37 (8) (2010) 5640–5644, https://doi.org/10.1016/j.eswa.2010.02.048.
[22] S. Kumar, A. Gupta, R.K. Bindal, Load-frequency and voltage control for power quality enhancement in a SPV/Wind utility-tied system using GA & PSO optimization, Results in Control and Optimization 100442 (2024), https://doi.org/10.1016/j.rico.2024.100442.
[23] W. Huang, H. Liu, Y. Zhang, R. Mi, C. Tong, W. Xiao, B. Shuai, Railway dangerous goods transportation system risk identification: comparisons among SVM, PSO-SVM, GA-SVM and GS-SVM, Appl. Soft Comput. 109 (2021) 107541, https://doi.org/10.1016/j.asoc.2021.107541.
[24] A. Bemani, Q. Xiong, A. Baghban, S. Habibzadeh, A.H. Mohammadi, M.H. Doranehgard, Modeling of cetane number of biodiesel from fatty acid methyl ester (FAME) information using GA-, PSO-, and HGAPSO-LSSVM models, Renew. Energy 150 (2020) 924–934, https://doi.org/10.1016/j.renene.2019.12.086.

[25] L. Wang, R. Xu, Multistart Nelder–Mead neural network algorithm for earthquake source parameter inversion of 2017 Bodrum–Kos earthquake, J. Survey Eng. 147 (3) (2021) 04021014, https://doi.org/10.1061/(ASCE)SU.1943-5428.0000368.
[26] L. Wang, R. Xu, F. Yu, Genetic Nelder-Mead neural network algorithm for fault parameter inversion using GPS data, Geodesy and Geodynamics 13 (4) (2022) 386–398, https://doi.org/10.1016/j.geog.2021.12.005.
[27] L. Wang, X. Luo, Adaptive Quasi-Monte Carlo method for nonlinear function error propagation and its application in geodetic measurement, Measurement 186 (2021) 110122, https://doi.org/10.1016/j.measurement.2021.110122.
[28] L. Wang, S. Han, M. Pang, Improved artificial gorilla troops optimizer with chaotic adaptive parameters-application to the parameter estimation problem of mixed additive and multiplicative random error models, Meas. Sci. Technol. 35 (2) (2023) 025203, https://doi.org/10.1088/1361-6501/ad093b.
[29] F. Aguirre, A. Sebastian, M. Le Gallo, W. Song, T. Wang, J.J. Yang, M. Lanza, Hardware implementation of memristor-based artificial neural networks, Nat. Commun. 15 (1) (2024) 1974, https://doi.org/10.1038/s41467-024-45670-9.
[30] K. Lu, J. Liang, M. Liu, Z. Lu, J. Shi, P. Xing, L. Wang, Research on transmission efficiency prediction of heavy-duty tractors HMCVT based on VMD and PSO–BP, Agriculture 14 (4) (2024) 539, https://doi.org/10.3390/agriculture14040539.
[31] Z. Tong, Y. Meng, J. Zhang, Y. Wu, Z. Li, D. Wang, G. Ou, Coal structure identification based on geophysical logging data: insights from wavelet Transform (WT) and particle swarm optimization support vector machine (PSO-SVM) algorithms, Int. J. Coal Geol. 282 (2024) 104435, https://doi.org/10.1016/j.coal.2023.104435.
[32] C. Ding, Y. Xia, Z. Yuan, H. Yang, J. Fu, Z. Chen, Performance prediction for a fuel cell air compressor based on the combination of backpropagation neural network optimized by genetic algorithm (GA-BP) and support vector machine (SVM) algorithms, Therm. Sci. Eng. Prog. 44 (2023) 102070, https://doi.org/10.1016/j.tsep.2023.102070.
[33] A.K. Rastogi, S. Taterh, B.S. Kumar, Original Research Article Hybrid GA-mSVM: dimensionality reduction using hybrid genetic algorithm and modified support vector machine classifier, Journal of Autonomous Intelligence 7 (3) (2024), https://doi.org/10.32629/jai.v7i3.799.
[34] H. Nadrian, H. Heizomi, S. Shirzadi, M.S. Moradi, P. Hajibadali, Exploring the dimensions of urban quality of life associated with urban traffic jam: the development and validation of an instrument, J. Transport Health 26 (2022) 101463, https://doi.org/10.1016/j.jth.2022.101463.
[35] J. Masaka, F. Sueyoshi, M.A. Hossain, S. Utsumi, J. Tanimoto, Can the introduction of CAVs mitigate social dilemmas causing traffic jams on highways? Physics Open 17 (2023) 100176 https://doi.org/10.1016/j.physo.2023.100176.
[36] Y. Han, H. Yu, Z. Li, C. Xu, Y. Ji, P. Liu, An optimal control-based vehicle speed guidance strategy to improve traffic safety and efficiency against freeway jam waves, Accid. Anal. Prev. 163 (2021) 106429, https://doi.org/10.1016/j.aap.2021.106429.
[37] Y. Kim, H.Y. Tak, S. Kim, H. Yeo, A hybrid approach of traffic simulation and machine learning techniques for enhancing real-time traffic prediction, Transport. Res. C Emerg. Technol. 160 (2024) 104490, https://doi.org/10.1016/j.trc.2024.104490.
[38] B.S. Kerner, S.L. Klenov, V. Wiering, M. Schreckenberg, A methodology of cooperative driving based on microscopic traffic prediction, Phys. Stat. Mech. Appl. 643 (2024) 129780, https://doi.org/10.1016/j.physa.2024.129780.
[39] Z. Zhu, M. Xu, J. Ke, H. Yang, X.M. Chen, A Bayesian clustering ensemble Gaussian process model for network-wide traffic flow clustering and prediction, Transport. Res. C Emerg. Technol. 148 (2023) 104032, https://doi.org/10.1016/j.trc.2023.104032.
[40] S. Manikandan, M. Chinnadurai, D.M.M. Vianny, D. Sivabalaselvamani, Real time traffic flow prediction and intelligent traffic control from remote location for large-scale heterogeneous networking using tensorflow, International Journal of Future Generation Communication and Networking 13 (1) (2020) 1006–1012.
[41] T.D. Toan, V.H. Truong, Support vector machine for short-term traffic flow prediction and improvement of its model training using nearest neighbor approach, Transport. Res. Rec. 2675 (4) (2021) 362–373, https://doi.org/10.1177/03611981209804.
[42] G.J. Tan, The structure method and application of background value in grey system GM (1, 1) model (I), Systems Engineering-Theory & Practice 20 (4) (2000) 98–103, https://doi.org/10.12011/1000-6788 (2000)4-98.
[43] Z.X. Wang, Y.G. Dang, S.F. Liu, Optimization of background value in GM (1, 1) model, Systems engineering-theory & practice 28 (2) (2008) 61–67, https://doi.org/10.1016/S1874-8651(09)60011-9.
[44] Z. Lihua, D. Suliang, J. Butterworth, X. Ma, B. Dong, A. Liu, Grey forecasting model for active vibration control systems, J. Sound Vib. 322 (4–5) (2009) 690–706, https://doi.org/10.1016/j.jsv.2008.11.036.
[45] Y.H. Lin, C.C. Chiu, P.C. Lee, Y.J. Lin, Applying fuzzy grey modification model on inflow forecasting, Eng. Appl. Artif. Intell. 25 (4) (2012) 734–743, https://doi.org/10.1016/j.engappai.2012.01.001.
[46] J.F. Li, W.Z. Dai, A new approach of background value-building and its application based on data interpolation and Newton-Cores formula, Systems Engineering Theory & Practice 24 (10) (2004) 122–126.
[47] F. Chen, Y. Zhu, A new GM (1, 1) based on piecewise rational linear/linear monotonicity-preserving interpolation spline, Eng. Lett. 29 (3) (2021).
[48] Y. Zhu, Z. Jian, Y. Du, W. Chen, J. Fang, A new GM (1, 1) model based on cubic monotonicity-preserving interpolation spline, Symmetry 11 (3) (2019) 420, https://doi.org/10.3390/sym11030420.
[49] M. Cheng, G. Shi, Improved methods for parameter estimation of gray model GM (1, 1) based on new background value optimization and model application, Commun. Stat. Simulat. Comput. 51 (2) (2022) 647–669, https://doi.org/10.1080/03610918.2019.1657450.
[50] X. Ma, W. Wu, Y. Zhang, Improved GM (1, 1) model based on Simpson formula and its applications, arXiv preprint arXiv (2019), https://doi.org/10.48550/arXiv.1908.03493, 1908.03493.
[51] W. Yuhong, L. Jie, Improvement and application of GM (1, 1) model based on multivariable dynamic optimization, J. Syst. Eng. Electron. 31 (3) (2020) 593–601, https://doi.org/10.23919/JSEE.2020.000024.
[52] C. Liu, T. Lao, W.Z. Wu, W. Xie, Application of optimized fractional grey model-based variable background value to predict electricity consumption, Fractals 29 (2) (2021) 2150038, https://doi.org/10.1142/S0218348X21500389.
[53] J.H. Wu, C.R. Lauh, A study to improve GM (1, 1) via heuristic method, J. Grey Syst. 10 (3) (1998) 183–192.
[54] Z.X. Wang, A genetic algorithm-based grey method for forecasting food demand after snow disasters: an empirical study, Nat. Hazards 68 (2013) 675–686, https://doi.org/10.1007/s11069-013-0644-8.
[55] M. Zhang, W. Xiao, Construct and realization of Newton interpolation polynomial based on Matlab7, Procedia Eng. 15 (2011) 3831–3835, https://doi.org/10.1016/j.proeng.2011.08.717.
[56] S. Mahmoudinazlou, C. Kwon, A hybrid genetic algorithm with type-aware chromosomes for traveling salesman problems with drone, Eur. J. Oper. Res. (2024), https://doi.org/10.1016/j.ejor.2024.05.009.
[57] C.H. Wang, L.C. Hsu, Using genetic algorithms grey theory to forecast high technology industrial output, Appl. Math. Comput. 195 (1) (2008) 256–263, https://doi.org/10.1016/j.amc.2007.04.080.
[58] S.P.T.P. Phyu, G. Srijuntongsiri, A binary coded multi-parent genetic algorithm for shuttle bus routing system in a college campus, in: 2016 International Conference on Advanced Informatics: Concepts, Theory and Application (ICAICTA), IEEE, 2016, August, pp. 1–5, https://doi.org/10.1109/ICAICTA.2016.7803089.
[59] R. Vallée, Grey information: theory and practical applications, Kybernetes 37 (1) (2008), https://doi.org/10.1108/03684920810851078, 189-189.